ANNALS OF FACULTY ENGINEERING HUNEDOARA
– INTERNATIONAL JOURNAL OF ENGINEERING
Tome X (Year 2012) – FASCICULE 3 (ISSN 1584 – 2673)

[1.] Liany Amelia HENDRATTA, [2.] Terunori OHMOTO

NON-NEWTONIAN PROPERTIES AND FLOW STRUCTURE IN HYPERCONCENTRATED SEDIMENT LADEN FLOWS

[1-2.] DEPARTMENT OF CIVIL AND ENVIRONMENTAL ENGINEERING, KUMAMOTO UNIVERSITY, JAPAN

ABSTRACT: *Mud flows, debris flows or slurries, made up of a large amount of clay and/or silt particles suspended in water, often show non-Newtonian properties but remain poorly understood concerning their rheological properties. This paper concerns an experimental study of the rheological properties of mudflows that were investigated by using coaxial cylinder. Shear stress and viscosity of the experimental results have relation with shear rate, sediment concentration, and temperature and particle size distribution. In addition the relation between shear stress and shear rate is described by Power law model at low shear rate that shear rate did not fit to Bingham model. It was clarified that the rheological properties of Poly sodium acrylic (PSA) solution was similar to mud flows.*
KEYWORDS: *non-Newtonian fluid, mudflows, rheological properties*

INTRODUCTION

A flow containing a high percentage of fine sediment or gravel may occur in the form of a mudflow or a debris flow. The Bingham model, which pays attention to yield stress, is often used to analyse shear characteristics of hyperconcentrated sediment-laden flows.

Yang et al. (1996) modified Einstein's viscosity formula for application to a water suspension of Yellow River sediment on the basis of the percentage content of 0.025 mm or smaller particles. Bradley and McCutcheon (1985) regarded water flow with a sediment content by volume of 20% or less as a standard water flow in which the influence on density and viscosity is small and pointed out that sediment-laden flows show their characteristics at a sediment content of 20% or more and a sediment-laden flow with a clay or silt content by volume of 5% or more shows non-Newtonian fluid properties. Coussot (1992) presented a relation between shear stress and the shear rate for hyperconcentrated sediment-laden flow by using a Herschel–Bulkley model with three parameters.

Concerning hyperconcentrated sediment-laden flow in an open channel, only a small number of studies have been conducted to obtain detailed measurement data on flow velocity changes because of the difficulty in measurement, and the influence of non-Newtonian fluid properties on resistance and the internal structure of flow remains poorly understood.

Huang and Garcia (1998) theoretically derived the vertical distribution of main flow velocity by assuming that flow is laminar and using the Herschel–Bulkley model. Fu (2005) treated fluid and solid separately, regarding sediment-laden flow as fluid–solid two-phase flow, and took into account the effects of fluid lift force and sediment stress gradient in considering the vertical distribution of sediment concentration.

In this study, an experiment was conducted in order to investigate the influence of hyperconcentrated sediment-laden flows on the friction characteristics of smooth-type beds of open channels and the structure of such flows. In the experiment, the flow field over a smooth bed was investigated in detail through comparison with clear water flow by using sodium polyacrylate (PSA) solutions with viscosity characteristics similar to those of hyperconcentrated sediment-laden flow and applying PIV (particle image velocimetry) to current meters. This study deals only with wash loads when considering hyperconcentrated sediment-laden flows and assumes that fine-grained sediment is not deposited on the channel bed and spatial changes in concentration distribution are small.

EXPERIMENTAL APPARATUS AND METHODS

The materials used for viscosity measurement are suspensions of the Yellow River sediment, suspensions of kaolin and PSA solutions used as polymer solutions.

Figure 1 shows the particle size distributions of Yellow River sediment (abbreviated as "YRS" in the figures) and kaolin.

The Yellow River sediment samples used were taken from Yellow River bed material in Jinan City located along the lower Yellow River in China. The median particle size of the Yellow River sediment was d_{50} = 16.2 μm, and that of the kaolin was d_{50} = 5.3 μm. As can be seen from the particle size distributions, the kaolin particles are fairly uniform in size,

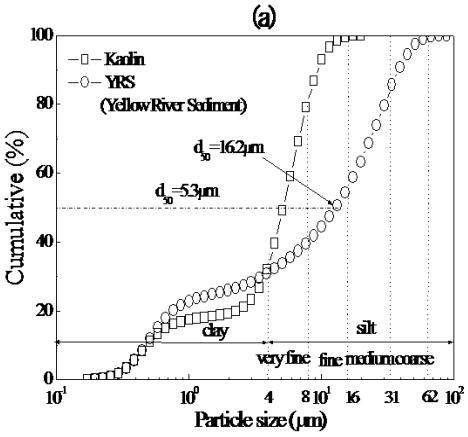

Fig 1. Grain size distributions

while the Yellow River sediment varies in size, which is a characteristic of natural sand.

For viscosity measurement, Brookfield's DV-II+ PRO Digital Viscometer, which excels in the measurement of viscosity at low shear rates, was used. Since the viscosity of non-Newtonian fluids is highly dependent on temperature, a well-insulated pipe was used to connect a constant-temperature circulating tank capable of keeping water temperature within about ±0.3°C during measurement was used to stably keep sample water temperature at 20°C.

The kaolin suspensions and PSA solutions used in the viscosity experiment were made to flow in a circulating variable-slope flume made of acrylic resin measuring 10 m in length, 0.4 m in width and 0.2 m in height. The experiment conditions are shown in Tables 2 and 3. Resistance was calculated by measuring water depth of a uniform flow field with gauges point. Also, for the purpose of checking on the uniformity of distribution of kaolin suspension concentration, samples were taken at four points located in the region from the bed surface to the water surface.

Hyperconcentrated sediment-laden flow can be reproduced by using a PSA solution as a simulant fluid. Flow velocity measurement was conducted, therefore, by applying PIV to open-channel flow of a PSA solution.

Table 1. Parameters in models

Cv (%)	Herschel Bulkley model			Power Law model	
	τc (Pa)	K (Pa.s^n)	n	η (Pa.s^n)	n
5.4	0.0005	0.0146	0.693	0.0150	0.688
6	0.0024	0.0400	0.552	0.0403	0.551
7	0.0082	0.0743	0.483	0.0713	0.491
8	0.0210	0.151	0.413	0.133	0.439
10	0.120	0.537	0.287	0.519	0.294

Table 2. Experimental conditions (Kaolin suspension)

	Cv (%)	Q (l/s)	Io	H (cm)	Um (cm/s)	Fr
Clear water	0	6.0	1/400	3.07	48.9	0.891
Kaolin suspension	5.04	6.0	1/400	3.15	47.6	0.857
	6.50	6.0	1/400	3.15	47.6	0.857
	7.33	6.0	1/400	3.23	46.4	0.825
	8.15	6.0	1/400	3.25	46.2	0.818
	9.38	6.0	1/400	4.15	36.1	0.567
	10.2	6.0	1/400	4.72	31.8	0.467
	11.3	6.0	1/400	5.30	28.3	0.393
	11.9	6.0	1/400	5.61	26.7	0.361

Table 3. Experimental conditions (PSA solution)

	Cw (mg/l)	Q (l/s)	Io	H (cm)	Um (cm/s)	Fr
W1	0	3.0	1/1000	2.53	29.6	0.595
P-a1	400	10.0	1/1000	5.20	48.1	0.674
P-b1	250	3.0	1/1000	2.62	28.6	0.565
P-b2	300	3.0	1/1000	2.63	28.5	0.562
P-b3	400	3.0	1/1000	2.65	28.3	0.555
P-b4	500	3.0	1/1000	2.85	26.3	0.498
P-b5	600	3.0	1/1000	3.02	24.5	0.448
P-b6	800	3.0	1/1000	3.50	21.4	0.366

The origin of the coordinate system was defined at the midpoint of the bottom of the flume where a uniform flow field was formed. The x-axis, y-axis and z-axis were defined as the stream direction, the cross-stream (transverse) direction and the vertical direction, respectively, and the respective flow velocity change components were represented by u, v and w. As a PIV light source, an air-cooled double-pulse YAG laser was used. The laser light sheet was set to a thickness of 1 mm, a width of 10 cm and a pulse interval of 1,000 μsec, and laser light was directed vertically upward from the flume bottom toward the water surface from the flume bottom midpoint located at y = 20 cm. Images of visualized particles passing through the laser light sheet were recorded in pairs with a CCD camera (Kodak Megaplus ES1.0; 1,008 × 1,008 pixels) installed on one of the sidewalls of the flume. Flow velocity sampling frequency was 15Hz, and 1,000 images were statistically processed for each measurement plane. Nylon particles 5 μm in diameter and having a specific gravity of 1.02 were used as tracers.

VISCOUS PROPERTIES

Particles in water coagulate by cohesion between them so that flocculation results. Such property of silt and clay in hyperconcentrated sediment-laden flow can cause considerable changes in the viscous properties of flow. In order to investigate the flow structure of hyperconcentrated sediment-laden flow, therefore, it is necessary first to identify its viscous properties. Parameters that characterize the viscous properties of hyperconcentrated sediment-laden flow include sediment concentration, particle size distribution and temperature.

Figure 2 shows the relationship between shear stress and the shear rate for 10% and 20% (C_v, i.e., volumetric concentration) kaolin suspensions. The dotted lines in the figure indicate the Bingham model shown in Eq. (1) for different volumetric concentrations.

$$\tau = \tau_y + \mu_B \left(du/dy \right) \quad (1)$$

where τ is shear stress; τ_y, yield stress; μ_B, apparent viscosity; and du/dy, the shear rate.

The horizontal axis in Fig. 2 shows the shear rate, and the vertical axis shows shear stress made dimensionless by the yield stress in the Bingham model. At shear rates of about 300 1/s or less, the relationship between shear stress and the shear rate is not linear, and the approximation curves of the Bingham model do not necessarily agree with measured values.

Figure3 shows the relationship between apparent viscosity and volumetric concentration. The horizontal axis shows the shear rate, and the vertical axis measures the apparent viscosity made dimensionless by the viscosity coefficient of clear water. As shown, apparent viscosity tends to decrease as the shear rate rises and tends to increase as volumetric concentration increases. With respect to the

apparent viscosity at Cv = 5.4%, the shear rate is 264 1/s, which is 2.6 times higher than that of clear water. At Cv = 10%, the shear rate is 6.6 1/s, which is about 136 times higher than that of clear water. The apparent viscosity of the Yellow River sediment suspension at Cv = 30% shows a tendency similar to that of the apparent viscosity of the kaolin suspension at Cv = 10%.

The Herschel–Bulkley model that takes into consideration yield stress as shown in Eq. (2):

$$\tau = \tau_y + k\left(du/dy\right)^n \tag{2}$$

where τ_y *is yield stress;* k *and* n *parameters; and* $k\left(du/dy\right)^{n-1}$ *, apparent viscosity.*

Figure 4 uses a power-law model that does not take yield stress into consideration as shown in Eq. (3):

$$\tau = \eta_0\left(du/dy\right)^n \tag{3}$$

where η_0 *and* n *are parameters, and* $\eta_0\left(du/dy\right)^{n-1}$ *is the apparent viscosity.*

Both models express the measured values with relatively good accuracy, and their parameters are shown in Table 1. The values of τ_y, k, η_0 *and* n *have been obtained from approximation curves, and* τ_y *is a value at a shear rate of 0.01 1/s . Since its values are very small (0.0005 Pa at* C_v *= 5.4 and 0.12 Pa at* C_v *= 10%), hereafter the power-law model, which uses a smaller number of parameters, is used for the purposes of this study.*

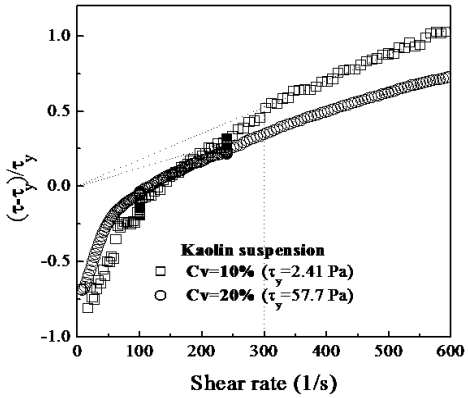

Fig 2. Application of Bingham model

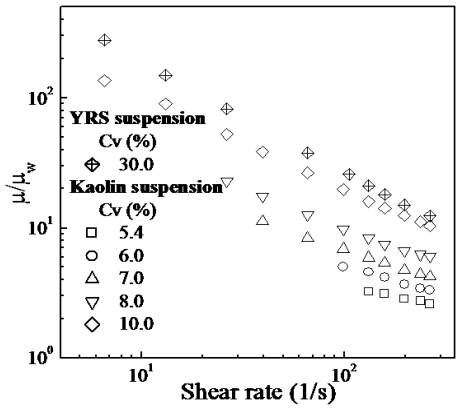

Fig 3. Relationship of apparent viscosity, shear rate and volumetric concentration

Power-law model shows the relationship of η_0 *and* n *with volumetric concentration in the power-law model. In the range of* C_v *from 5.4% to 10%,* η_o *increases exponentially as volumetric concentration increases. Conversely,* n *tends to decrease linearly as volumetric concentration increases. The dependence of each parameter on the volumetric concentration* C_v *is approximated by Eq. (4) and Eq. (5):*

$$\eta_0 = 0.00993e^{Cv/1.59} \tag{4}$$

$$n = 1.04 - 0.00772Cv \tag{5}$$

As can be seen from Fig. 5, agreement in this relationship is good in the range of C_v *from 5.4% to 10%.*

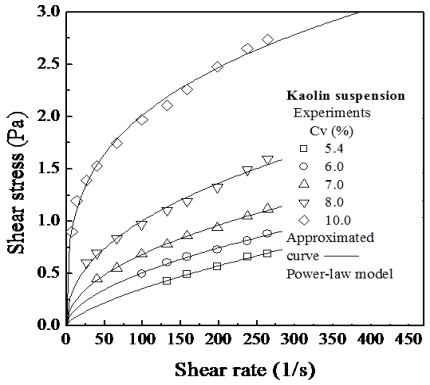

Fig 4. Application of a power-law model to kaolin suspension

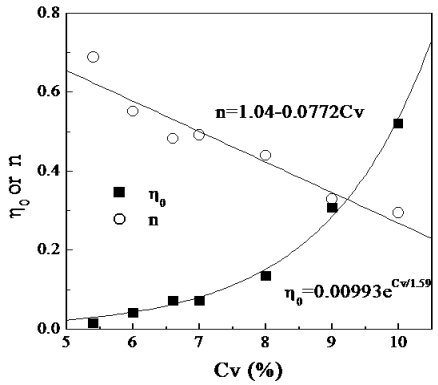

Fig 5. Parameters η_o *and n in power-law model*

RESISTANCE PROPERTIES

In the area of ordinary suspended sediment flows, concerning the resistance of hyperconcentrated sediment-laden flow, Yang,C.T. and X.Kong(1991) reported that in a smooth open-channel flow experiment using silt having a median grain size d_{50}*= 0.026 mm, resistance increased with*

sediment concentration. Also, Wang (1993) reported that in an experiment conducted by using clay, volumetric concentration somewhat increased at about 9%. So far, however, no systematic measurement data have been obtained on sediment-laden flows containing high concentrations of clay or silt, and consensus is yet to be reached as to the increase or decrease in resistance due to increases in concentration.

Figure 6 shows the relationship between the total resistance coefficient and concentration in the flume experiments in which kaolin suspensions and PSA solutions were used. The total resistance coefficient is defined as the ratio of total resistance to the inertia force of the fluid and can be expressed as

$$C_f = 2\left(U_*/U_m\right)^2 \tag{6}$$

where $U_*=\sqrt{ghi_0}$ *; g gravitational acceleration;* i_0 *channel flume slope; and* U_m *cross-sectionally averaged flow velocity. The vertical axis in the figure shows the ratio of the total resistance coefficient of the kaolin suspension,* C_{fK}*, to the total resistance coefficient of clear water,* C_{fW}*, i.e.,* C_{fK}/C_{fW}*, and the ratio of the total resistance coefficient of the PSA solution,* C_{fPSA}*, to* C_{fW}*, i.e.,* C_{fPSA}/C_{fW}*. As shown, the resistance coefficient* C_{fK}/C_{fW} *changed within the range from 1.08 to 6.10. Significant changes did not occur in a kaolin suspension in the range of* C_v *= 5.04 to 8.15%, and a linear increase tendency was observed in the range of* C_v *= 8.15 to 11.9%. This tendency of the resistance coefficient to increase with volumetric concentration is close to the pipe flow experiment result obtained by Ohmoto et al. (2004) and the result reported by Egashira et al.(1992)[2] to the effect that in an open channel experiment conducted using fine sand, resistance increased as transported sediment concentration increased. As shown, the total resistance coefficient of the flow of the PSA solution used as a simulant fluid tends to rise sharply at a PSA solution concentration of 400 mg/l or more. It can also be seen that this tendency to increase resembles the resistance properties of hyperconcentrated sediment-laden flow reproduced by using kaolin.*

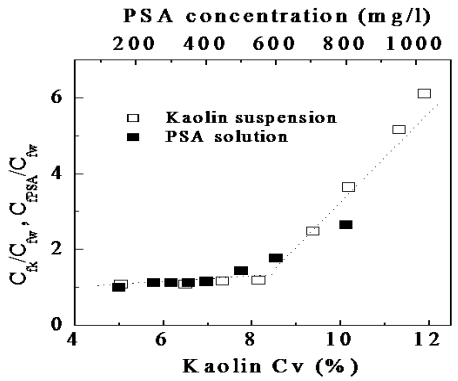

Fig 6. Relationship between flow resistance and concentration

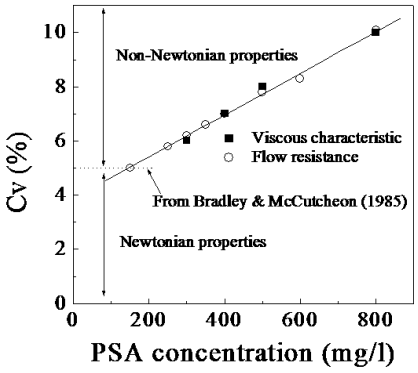

Fig 7. PSA solution equivalent to kaolin suspension

FLOW STRUCTURE OF PSA SOLUTION – SIMILARITY OF HYPERCONCENTRATED SEDIMENT-LADEN FLOW AND PSA SOLUTION

As mentioned in Chapters 2 and 3, kaolin suspensions and PSA solutions show similar tendencies in terms of non-Newtonian fluid properties and open-channel resistance properties. The relationship between the sediment concentration of the kaolin suspension and the concentration of the PSA solution shown in Fig. 7 was obtained by extracting concentrations at which non-Newtonian fluid properties show a high degree of similarity and concentrations at which resistance properties show a high degree of similarity from Fig. 6. It can be seen that under the experimental conditions, the concentrations of the kaolin suspension and the PSA solution are linearly related in terms of non-Newtonian fluid properties and resistance properties. Since, however, non-Newtonian fluid properties are not likely to be observable[3] when the sediment concentration by volume of the kaolin suspension is 5% or less, the linear relationship mentioned above holds true only when the volumetric concentration of sediment is 5% or more (Bradley, J. B. and McCutcheon, S.C(1985)).

MAIN FLOW VELOCITY AND SHEAR RATE DISTRIBUTIONS

Figure 8 shows the vertical distribution of the values obtained by making main flow velocity dimensionless by the maximum flow velocity U_{max}*. As shown, in Cases P-a1, P-b1 and P-b2, the main flow velocity distributions are close to those of clear water flow. In P-b3 to P-b6, the distributions differ considerably from those of clear water flow; main flow velocity is kept low in the near-bottom zone, and the distributions show gentle curves. The fact that the spatial distribution of main flow velocity changes sharply as the concentration of the PSA solution increases from 300 mg/l to 400 mg/l indicates that the internal structure of flow has changed substantially.*

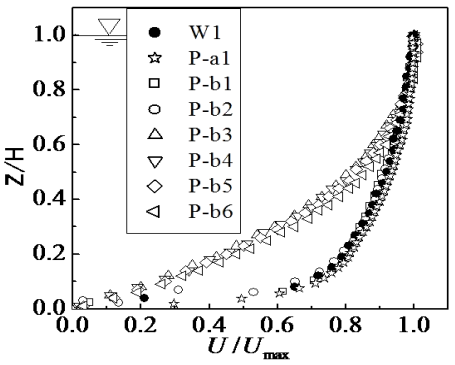

Fig 8. Main flow velocity

A possible main cause of the substantial difference in the spatial distribution of main flow velocity is a considerable change in the mode of momentum transport.

To be more specific, when the flow was close to clear water flow, it was in a state of turbulence, and as the concentration of the PSA solution increased, a transition may have occurred from turbulent flow to laminar flow. The Reynolds number, which is an indicator of the type of flow field, cannot be calculated easily because in the case of a non-Newtonian fluid, kinematic viscosity is not a property but a state variable dependent on the shear rate.

TURBULENCE CHARACTERISTICS AND REYNOLDS STRESS

Figures 9 and 10 show the vertical distributions of streamwise turbulence intensity u_{rms} *and vertical turbulence intensity* w_{rms}.

Figure 11 shows the vertical distribution of the Reynolds stress $-\overline{u'w'}$. *Turbulence intensity and the Reynolds stress tend to decrease as the concentration of the PSA solution increases. In Case P-b3 to Case P-b6, in which the vertical distribution of main flow velocity differed considerably from that of clear water flow, changes in the vertical direction are small both in turbulence intensity and the Reynolds stress, and the Reynolds stress is close to zero. This indicates that although the flow field influences and is influenced by kinematic viscosity and kinematic eddy viscosity, viscous stress becomes the dominant resistance component if the kinematic viscosity at the bottom is greater than that of clear water flow by a factor of 10 or more so that the flow field becomes laminar. This is consistent with the results related to resistance properties.*

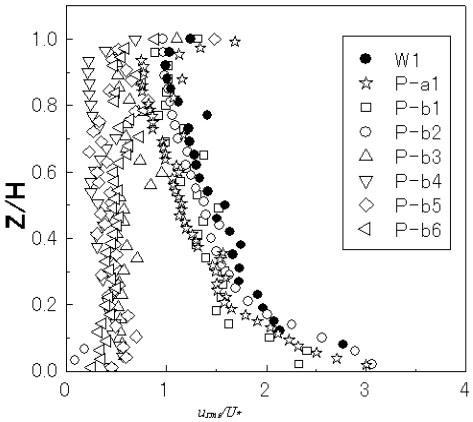

Fig 9. Vertical distribution of u_{rms}/U_*

LAMINAR FLOW AND TURBULENT FLOW VELOCITY DISTRIBUTIONS

Figure 12 shows the vertical component of main flow velocity under the experiment conditions, where $U^+=U/U_*$, $Z^+=Z\square U_*/\nu$, $U_*=\sqrt{\tau_0/\rho}$, $\tau_0=\mu\left(dU/dZ|_{Z=0}\right)$, $\nu=\mu/\rho$, *and* $\mu=\eta_0\left(dU/dZ|_{Z=0}\right)^n$.

The broken line in Fig. 6 is the maximum drag reduction curve proposed by Virk (1971). In Cases P-a1, P-b1 and P-b2, in which flow is not laminar, approximation can be made according to the logarithmic law in the region at a height of $Z^+>30$. *In Case P-b3, in which the flow became laminar, the apparent Karman constant* κ *decreased, and as Virk's maximum drag reduction curve became closer and the concentration of the PSA solution continued to increase, the apparent Karman constant* κ *showed a tendency to increase. In the case of clear water flow, the velocity of laminar flow is distributed within the range of* $Z^+<30$, *which corresponds to the viscous sublayer and the buffer layer.*

The distribution of laminar flow velocity can be determined theoretically, and can be calculated by using the Bingham model as

$$U = U_p\left(1-z/h_s\right)^2 \qquad (7)$$

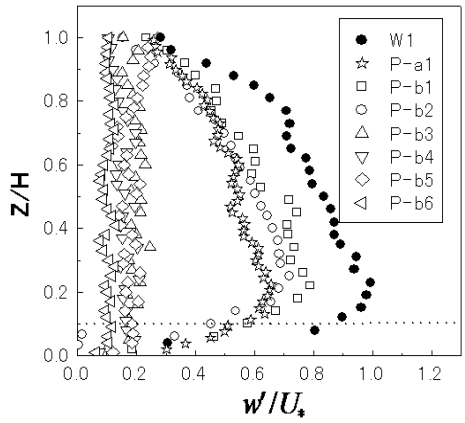

Fig 10. Vertical distribution of w_{rms}/U_*

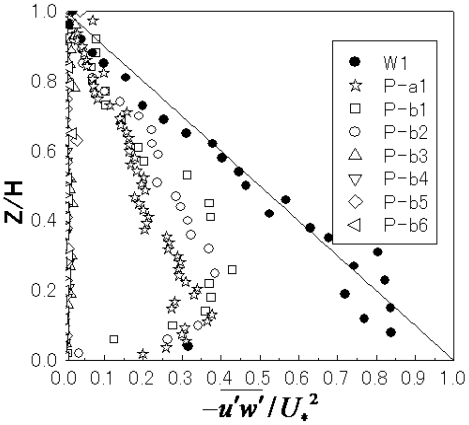

Fig.11 Vertical distribution of $-u'w'/U_*^2$

where U *is the main flow velocity;* U_p, *flow velocity in the plug layer;* $h_S=H-h_p$, *thickness of the shear layer;* H, *water depth; and* h_p, *thickness of the plug layer. If the power-law model is used, the flow velocity distribution can be calculated as*

$$U=U_{\max}\left(1-z/H\right)^{(n+1)/n} \qquad (8)$$

where $U_{\max}$ *is the maximum main flow velocity; and* n, *a viscosity parameter of the power-law model. Figure 13 shows the measured main flow velocities in Case P-b6 and the calculated values obtained from Eq. (7) and Eq. (8). As shown, the calculated values obtained from the power-law model show good agreement with the measured values. The degree of agreement of the calculated values obtained from the Bingham model, however, is lower, and the measured values do not indicate the existence of the plug layer inferred from the Bingham model.*

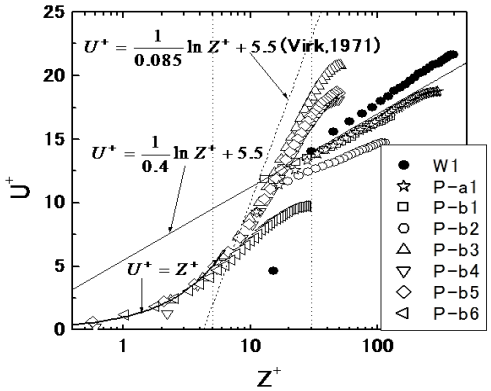

Fig.12.Logarithmic distribution of main flow velocity

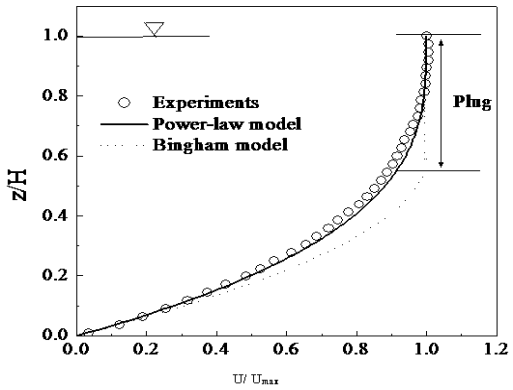

Fig.13. Vertical distribution of main flow velocity (laminar flow)

CONCLUSIONS

This study has investigated the viscous properties and resistance properties of hyperconcentrated sediment-laden flows and PSA solution flows in detail in order to elucidate the internal structure of hyperconcentrated sediment-laden flow by using a PSA solution capable of simulating hyperconcentrated sediment-laden flow. The knowledge gained from this study is listed as follows:

(1) It has been shown that non-Newtonian fluid properties of hyperconcentrated sediment-laden flow can be expressed with the power-law model, and its parameters, namely, η_0 and n, have been expressed as a function of the volumetric concentration of sediment.

(2) The kinematic viscosities of PSA solutions having concentrations of 300 mg/l, 400 mg/l, 500 mg/l and 800 mg/l show non-Newtonian fluid properties similar to the kinematic viscosities of kaolin suspensions having volumetric concentrations (C_v) of 6%, 7%, 8% and 10%, respectively.

(3) The total resistance coefficient of the flow of a PSA solution used as a simulant fluid showed a tendency to increase sharply at PSA solution concentrations of 400 mg/l or more, and the tendency of such increase held semblance to the resistance properties of hyperconcentrated sediment-laden flows produced by use of kaolin.

(4) Overall, turbulence intensity and the Reynolds stress tended to decrease as the concentration of the PSA solution increased. In Case P-b3 to Case P-b6, in which the vertical distribution of main flow velocity differed considerably from that of clear water flow, changes in the vertical direction were very small, compared with clear water flow, both in turbulence intensity and the Reynolds stress and were uniform in the vertical direction. Also, the Reynolds stress was close to zero, and the flow field was laminar.

(5) The calculated values obtained from the power-law model agreed well with the measured velocities in laminar flows. The calculated values obtained from the Bingham model showed a lower degree of agreement with the measured values, and the measured values did not indicate the existence of the plug layer inferred from the Bingham model.

(6) In Cases P-a1, P-b1 and P-b2, in which flow is not laminar, approximation, can be made according to the logarithmic law in the region at a height of $Z^+ > 30$, but resistance is higher than in clear water flow. This is thought to be due to the influence of non-Newtonian fluid properties, but details of such influence are to be addressed in a separate study.

REFERENCES

[1.] Bradley, J. B. and McCutcheon, S.C: The effect of high sediment concentration on transport processes and flow Phenomena, proc. Conf. Erosion, Debris prevention, Japan,1985.

[2.] Coussot, P.: Rheology of debris flow-Study of concentrated suspensions. Ph.D.thesis, INPG, Grenoble, France, 1992.

[3.] Egashira S., Ashida K., Tanonaka S. and Sato T.: Studies on Mud Flow-Stress Structure-, Annuals, Disas. Prev.Res. Inst.,Kyoto Univ. No.35,B-2, pp79-88,1992.

[4.] Ohmoto T., Cui Z. and Kakihara Y.: On Rheology of Hyperconcentrated Sediment-laden Flow, Journal of Applied Mechanics, JSCE, Vol.7, pp979-986, 2004.

[5.] Virk,P.S.: An Elastic Sublayer Model for Drag Reduction by Dilute Polymer Solutions, J.Fluid. Mech, Vol.45, pp417-440, 1971.

[6.] Xin Huang and Marcelo H. Garcia A.: Herschel-Bulkley model for mud flow down a slope. J.Fluid. Mech. vol374, pp305-333, 1998.

[7.] Xudong Fu.: Vertical Dispersion of Fine and Coarse Sediments in Turbulent Open-Channel Flows. J. Hydraulic Engineering. ASCE. pp. 877-888, October. 2005.

[8.] Yang, C.T. and X. Kong.: Energy Dissipation Rate and Sediment Transport, Journal of Hydraulic Research, Vol.29, no.4, pp.457-474, 1991.

[9.] Yang. C.T.: Sediment Transport in the Yellow River, Journal of Hydraulic Engineering, Vol.122, 2004, pp237-244, 1996.

[10.] Z.Y. Wang: A study on debris flow surges, Hydraulic Engineering'93, Vol.2, American Society of Civil Engineers, New York, pp. 1616-1621, 1993.